Stochastic Modeling and Simultaneous Regulation of Surface Roughness and Porosity in Thin Film Deposition

Gangshi Hu,[†] Gerassimos Orkoulas,[†] and Panagiotis D. Christofides*[,†,‡]

Department of Chemical and Biomolecular Engineering and Department of Electrical Engineering, University of California, Los Angeles, California 90095

This work focuses on stochastic modeling and simultaneous regulation of surface roughness and porosity for a porous thin film deposition process modeled via kinetic Monte Carlo (kMC) simulation on a triangular lattice. The microscopic model of the thin film growth process includes adsorption and migration processes. Vacancies and overhangs are allowed inside the film for the purpose of modeling thin film porosity. The definition of the surface height profile is first introduced for a porous thin film deposition taking place in a triangular lattice. The dynamics of surface height of the thin film are described by an Edwards-Wilkinson (EW) type equation, which is a second-order linear stochastic partial differential equation (PDE). The root-mean-square (RMS) surface roughness is chosen as one of the controlled variables. Subsequently, an appropriate definition of film site occupancy ratio (SOR) is introduced to represent the extent of porosity inside the film and is chosen as the second to-be-controlled variable. A deterministic ordinary differential equation (ODE) model is postulated to describe the time evolution of the film SOR. The coefficients of the EW equation of surface height and of the deterministic ODE model of the film SOR are estimated on the basis of data obtained from the kMC simulator of the deposition process using least-squares methods, and their dependence on substrate temperature is determined. The developed dynamic models are used as the basis for the design of a model predictive control algorithm that includes a penalty on the deviation of the surface roughness square and film SOR from their respective set-point values. Simulation results demonstrate the applicability and effectiveness of the proposed modeling and control approach in the context of the deposition process under consideration. When simultaneous control of surface roughness and porosity is carried out, a balanced trade-off is obtained in the closed-loop system between the two control objectives of surface roughness and porosity regulation.

1. Introduction

Thin film deposition processes play an important role in the semiconductor industry. In recent years, increasing complexity and density of microelectronic devices on wafers require significant improvement of thin film deposition process operation and yield. Thin film microstructure, including surface roughness and film porosity, strongly affects the electrical and mechanical properties of the thin films and of the resulting devices. Failure to manufacture thin films with the desired microstructure can only be detected at the end of the manufacturing process which results in high costs. Therefore, it is necessary to develop real-time monitoring and feedback control of thin film deposition processes.

Motivated by recent development of measurement techniques for online surface roughness measurements,[1−3] recent research efforts on modeling and control of thin film microstructure have been focused mostly on thin film surface roughness on the basis of microscopic thin film growth models which utilize a square lattice. Specifically, kinetic Monte Carlo (kMC) models based on a square lattice and utilizing the solid-on-solid (SOS) approximation for deposition were initially employed to develop an effective methodology to describe the evolution of film microstructure and design feedback control laws for thin film surface roughness.[4−6] This control methodology was successfully applied via computer simulations to surface roughness control of the following: (a) a gallium arsenide (GaAs) deposition process[7] and (b) a multispecies deposition process with long-range interactions.[8] Furthermore, a method that couples partial differential equation (PDE) models and kMC models was developed for computationally efficient multiscale optimization of thin film growth.[9] However, kMC models are not available in closed-form, and this limitation restricts the use of kMC models for system-level analysis and design of model-based feedback control systems. To overcome this problem, model identification of linear deterministic models from outputs of kMC simulators was used for controller design using linear control theory.[10−12] However, deterministic models are only effective in controlling the expected values of macroscopic variables, i.e., the first-order statistical moments of the microscopic distribution. For higher statistical moments of the microscopic distributions such as the surface roughness (the second moment of height distribution on a lattice), deterministic models may not be sufficient, and stochastic differential equation (SDE) models may be needed.

While the evolution of surface morphology of ultrathin films in several thin film preparation processes can be modeled by SDEs (this point has been demonstrated theoretically, computationally,[13−17] and experimentally),[18−20] the construction of SDE models from kMC simulation data or experimental data is not a trivial task. With respect to previous results on parameter estimation for stochastic dynamic models, early results on the analysis, parameter optimization, and optimal stochastic control for linear stochastic ordinary differential equation (ODE) systems can be found in the work by Åström.[21] More recently, likelihood-based methods for parameter estimation of stochastic ODE models have been developed.[22,23] In the context of parameter estimation for stochastic PDEs, recent results[24−27]

* To whom correspondence should be addressed. Tel.: +1(310)794-1015. Fax: +1(310)206-4107. E-mail: pdc@seas.ucla.edu.
[†] Department of Chemical and Biomolecular Engineering.
[‡] Department of Electrical Engineering.

10.1021/ie900708v CCC: $40.75
Published on Web 06/18/2009

employed statistical moments to reformulate the parameter estimation problem into one involving deterministic differential equations. The stochastic moments include the expected value and variance/covariance obtained from the data set generated by kMC simulations or obtained from experiments. Thus, the issue of parameter estimation of stochastic models could be addressed by employing parameter estimation techniques for deterministic systems. In the context of control of thin film surface roughness in square lattice models, systematic controller design methods based on linear[28,25,24,29] and nonlinear[26,30] SDE models have been developed, covering both state feedback and output feedback control considerations. These methods have been applied to modeling and surface roughness control in deposition and sputtering processes defined on a square lattice via simulations.

In the context of modeling of thin film porosity, kMC models have been widely used to model the evolution of porous thin films in many deposition processes, such as the molecular beam epitaxial (MBE) growth of silicon films and copper thin film growth.[31,32] Both monocrystalline and polycrystalline kMC models have been developed and simulated.[33,34] The influence of the macroscopic parameters, i.e., the deposition rate and temperature, on the porous thin film microstructure has also been investigated using kMC simulators of deposition processes. Deterministic and stochastic ODE models of film porosity were recently developed[35] to model the evolution of film porosity and its fluctuation and design model predictive control (MPC) algorithms to control film porosity to a desired level and reduce run-to-run porosity variability. Despite recent significant efforts on modeling and control of surface roughness and film porosity, simultaneous regulation of surface roughness and film porosity within a unified control framework has not been investigated.

Motivated by these considerations, the present work focuses on stochastic modeling and simultaneous regulation of surface roughness and film porosity in a porous thin film deposition process modeled via kMC simulation on a triangular lattice. The microscopic model of the thin film growth process includes adsorption and migration processes. Vacancies and overhangs are allowed inside the film for the purpose of modeling thin film porosity. The definition of surface height profile is first introduced for a porous thin film deposition taking place in a triangular lattice. The dynamics of surface height of the thin film are described by an Edwards-Wilkinson (EW) type equation, which is a second-order linear stochastic PDE model. The root-mean-square (RMS) surface roughness is chosen as one of the controlled variables. Subsequently, an appropriate definition of film site occupancy ratio (SOR) is introduced to represent the extent of porosity inside the film and is chosen as the second to-be-controlled variable. A deterministic ODE model is postulated to describe the time evolution of film SOR. The coefficients of the EW equation of surface height and of the deterministic ODE model of film SOR are estimated on the basis of data obtained from the kMC simulator of the deposition process using least-squares methods, and their dependence on substrate temperature is determined. The developed dynamic models are used as the basis for the design of a model predictive control algorithm that includes penalty on the deviation of surface roughness square and film SOR from their respective set-point values. Simulation results demonstrate the applicability and effectiveness of the proposed modeling and control approach in the context of the deposition process under consideration.

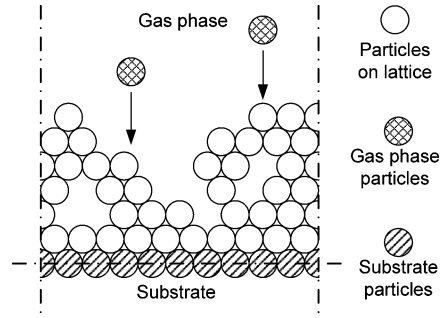

Figure 1. Thin film growth process on a triangular lattice.

2. Thin Film Deposition Process

2.1. Description and Modeling. The thin film growth process considered in this work includes two microscopic processes: an adsorption process, in which particles are incorporated into the film from the gas phase, and a migration process, in which surface particles move to adjacent sites.[31,33,34,36] Solid-on-solid (SOS) deposition models, in which vacancies and overhangs are forbidden, are frequently used to model thin film deposition processes[8,26] and investigate the surface evolution of thin films. However, vacancies and overhangs must be incorporated in the process model to account for film porosity. Since SOS models are inadequate to model the evolution of thin film internal microstructure, a ballistic deposition model taking place in a triangular lattice is chosen to simulate the evolution of film porosity. Below, we discuss the main aspects of this thin film growth process; more details can be found in ref 35.

The film growth model used in this work is an on-lattice kMC model in which all particles occupy discrete lattice sites. The on-lattice kMC model is valid for temperatures $T < 0.5T_m$, where T_m is the melting point of the crystal.[31] All particles are modeled as identical hard disks and the centers of the particles deposited on the film are located on the lattice sites. The diameter of the particles equals the distance between two neighboring sites. The width of the lattice is fixed so that the lattice contains a fixed number of sites in the lateral direction. The new particles are always deposited from the top side of the lattice where the gas phase is located; see Figure 1. Particle deposition results in film growth in the direction normal to the lateral direction. The direction normal to the lateral direction is thus designated as the growth direction. The number of sites in the lateral direction is defined as the lattice size and is denoted by L. The lattice parameter, a, which is defined as the distance between two neighboring sites and equals the diameter of a particle (all particles have the same diameter), determines the lateral extent of the lattice, La.

The number of nearest neighbors of a site ranges from zero to six, the coordination number of the triangular lattice. A site with no nearest neighbors indicates an unadsorbed particle in the gas phase (i.e., a particle which has not been deposited on the film yet). A particle with six nearest neighbors is associated with an interior particle that is fully surrounded by other particles and cannot migrate. A particle with one to five nearest neighbors is possible to diffuse to an unoccupied neighboring site with a probability that depends on its local environment. In the triangular lattice, a particle with only one nearest neighbor is considered unstable and is subject to instantaneous surface relaxation. Details of particle surface relaxation and migration will be discussed below.

In the simulation, a bottom layer in the lattice is initially set to be fully packed and fixed, as shown in Figure 1. There are

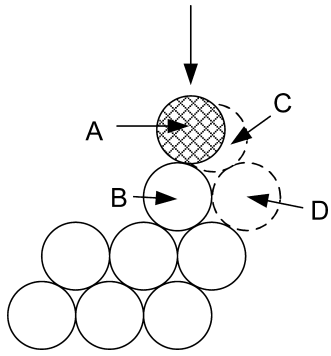

Figure 2. Schematic of the adsorption event with surface relaxation. In this event, particle A is the incident particle, particle B is the surface particle that is first hit by particle A, site C is the nearest vacant site to particle A among the sites that neighbor particle B, and site D is a stable site where particle A relaxes.

no vacancies in this layer, and the particles in this layer cannot migrate. This layer acts as the substrate for the deposition and is not counted in the computation of the number of the deposited particles, i.e., this fixed layer does not influence the film porosity (see section 2.2 below). Two types of microscopic processes (Monte Carlo events) are considered: an adsorption process and a migration process.

In the adsorption process, an incident particle comes in contact with the film and is incorporated onto the film. The microscopic adsorption rate, W, which is in units of layers per unit time, depends on the gas phase concentration. The layers in the unit of adsorption rate are densely packed layers, which contain L particles. With this definition, W is independent of L. In this work, the macroscopic adsorption rate, W, is treated as a process parameter. For the entire deposition process, the microscopic adsorption rate in terms of incident particles per unit time, which is denoted as r_a, is related to W as follows:

$$r_a = LW \tag{1}$$

The incident particles are initially placed at random positions above the film lattice and move toward the lattice in the vertical direction, as shown in Figure 1. The random initial particle position, x_0, which is the center of an incident particle, follows a uniform probability distribution in the continuous domain, $(0, La)$. The procedure of an adsorption process is illustrated in Figure 2. After the initial position is determined, the incident particle, A, travels along a straight line toward the film until contacting the first particle, B, on the film (this is a main difference compared to the process considered in ref 35 where the particle angle of incidence to the surface is allowed to vary and this leads to substantially different process physics and porosity patterns). Upon contact, particle A stops and sticks to particle B at the contacting position; see Figure 2. Then, particle A moves (relaxes) to the nearest vacant site, C, among the neighboring sites of particle B. Surface relaxation is conducted if site C is unstable, i.e., site C has only one neighboring particle, as shown in Figure 2. When a particle is subject to surface relaxation, the particle moves to its most stable neighboring vacant site, which is defined as the site with the most nearest neighbors. In the case of multiple neighboring vacant sites with the same number of nearest neighbors, a random one is chosen from these sites with equal probability as the objective of the particle surface relaxation process. Note that particle surface relaxation is considered as part of the deposition event, and thus, it does not contribute to the process simulation time. There is also only one relaxation event per incident particle.

In the migration process, a particle overcomes the energy barrier of the site and jumps to its vacant neighboring site. The migration rate (probability) of a particle follows an Arrhenius-type law with a precalculated activation energy barrier that depends on the local environment of the particle, i.e., the number of the nearest neighbors of the particle chosen for a migration event. The migration rate of the ith particle is calculated as follows:

$$r_{m,i} = \nu_0 \exp\left(-\frac{n_i E_0}{k_B T}\right) \tag{2}$$

where ν_0 denotes the pre-exponential factor, n_i is the number of the nearest neighbors of the ith particle and can take values of 2, 3, 4, and 5 ($r_{m,i}$ is zero when $n_i = 6$ since this particle is fully surrounded by other particles and cannot migrate), E_0 is the contribution to the activation energy barrier from each nearest neighbor, k_B is the Boltzmann constant, and T is the substrate temperature of the thin film. Since the film is thin, the temperature is assumed to be uniform throughout the film and is treated as a time-varying but spatially invariant process parameter. In this work, the factor and energy barrier contribution in eq 2 take the following values $\nu_0 = 10^{13}$ s^{-1} and $E_0 = 0.6$ eV, which are appropriate for a silicon film.[37] When a particle is subject to migration, it can jump to either of its vacant neighboring sites with equal probability, unless the vacant neighboring site has no nearest neighbors, i.e., the surface particle cannot jump off the film and it can only migrate on the surface.

The above-described thin film growth process has been simulated using a continuous-time Monte Carlo (CTMC) method via periodic boundary conditions (PBCs).[38] The details of the simulation algorithm can be found in ref 35; the reader may also refer to refs 39−42 for more details on Monte Carlo simulation algorithms.

2.2. Definitions of Surface Roughness and Film Site Occupancy Ratio. Utilizing the continuous-time Monte Carlo algorithm, simulations of the kMC model of a porous silicon thin film growth process are carried out. Snapshots of film microstructure, i.e., the configurations of particles within the triangular lattice, are obtained from the kMC model at various time instants during process evolution. To quantitatively evaluate the thin film microstructure, two variables, surface roughness and film porosity, are introduced in this subsection.

Surface roughness, which measures the texture of thin film surface, is represented by the root-mean-square (RMS) of the surface height profile of the thin film. Determination of a surface height profile is different in the triangular lattice model compared to an SOS model. In the SOS model, the surface of a thin film is naturally described by the positions of the top particles of each column. In the triangular lattice model, however, due to the existence of vacancies and overhangs, the definition of film surface needs further clarification. Specifically, taking into account practical considerations of surface roughness measurements, the surface height profile of a triangular lattice model is defined based on the particles that can be reached in the vertical direction, as shown in Figure 3. In this definition, a particle is considered as a surface particle only if it is not blocked by the particles of both of its neighboring columns. Therefore, the surface height profile of a porous thin film is the line that connects the sites that are occupied by the surface particles. With this definition, the surface height profile can be treated as a function of the spatial coordinate. Surface roughness, as a measurement of the surface texture, is defined as the standard deviation of the surface height profile from its average height. The mathematical expression of surface roughness is given later in section 3.1.

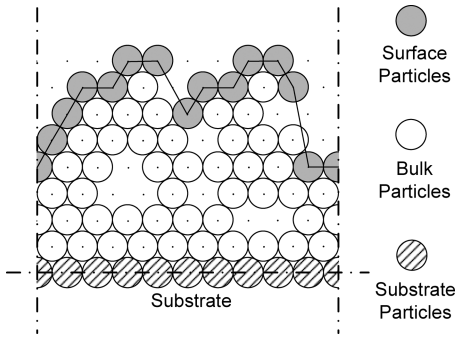

Figure 3. Definition of surface height profile. A surface particle is a particle that is not blocked by particles from both of its neighboring columns in the vertical direction.

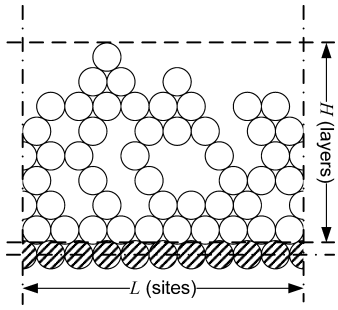

Figure 4. Illustration of the definition of the film SOR of eq 3.

In addition to film surface roughness, the film site occupancy ratio (SOR) is introduced to represent the extent of the porosity inside the thin film. The mathematical expression of the film SOR is defined as follows:

$$\rho = \frac{N}{LH} \tag{3}$$

where ρ denotes the film SOR, N is the total number of deposited particles on the lattice, L is the lattice size, and H denotes the number of deposited layers. Note that the deposited layers are the layers that contain only deposited particles and do not include the initial substrate layers. The variables in the definition expression of eq 3 can be found in Figure 4. Since each layer contains L sites, the total number of sites in the film that can be contained within the H layers is LH. Thus, film SOR is the ratio of the occupied lattice sites, N, over the total number of available sites, LH. The film SOR ranges from 0 to 1. Specifically, $\rho = 1$ denotes a fully occupied film with a flat surface. The value of zero is assigned to ρ at the beginning of the deposition process since there are no particles deposited on the lattice.

It is important to note that film surface roughness and porosity are correlated to some extent in the deposition process. A film with lower porosity tends to have a smoother surface, since the conditions to produce a dense film (higher substrate temperature or lower adsorption rate) also help reduce the surface roughness and vice versa. However, even though they are related to each other, roughness and porosity are separate variables that describe different aspects of the thin film. Films with the same film site occupancy ratio may have different surface roughnesses.

3. Dynamic Model Construction and Parameter Estimation

3.1. Edwards-Wilkinson-type Equation of Surface Height. An EW-type equation, a second-order stochastic PDE, can be used to describe the surface height evolution in many microscopic processes that involve thermal balance between adsorption (deposition) and migration (diffusion). In this work, an EW-type equation is chosen to describe the dynamics of the fluctuation of surface height (the validation of this choice will be made clear below):

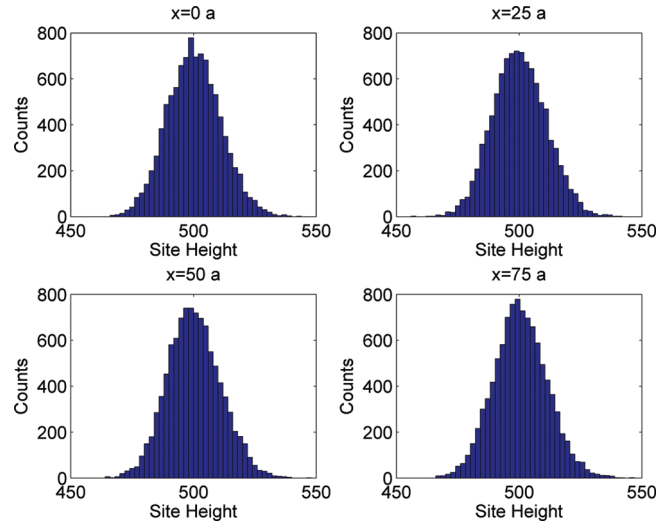

Figure 5. Histogram of surface height at different sites ($x = 0a$, $25a$, $50a$, $75a$) at $t = 400$ s.

$$\frac{\partial h}{\partial t} = r_h + \nu \frac{\partial^2 h}{\partial x^2} + \xi(x,t) \tag{4}$$

subject to PBCs

$$h(-\pi,t) = h(\pi,t), \quad \frac{\partial h}{\partial x}(-\pi,t) = \frac{\partial h}{\partial x}(\pi,t) \tag{5}$$

and the initial condition

$$h(x,0) = h_0(x) \tag{6}$$

where $x \in [-\pi,\pi]$ is the projected spatial coordinate, t is the time, r_h and ν are the model parameters, and $\xi(x,t)$ is a Gaussian white noise with the following expressions for its mean and covariance

$$\begin{aligned} \langle \xi(x,t) \rangle &= 0 \\ \langle \xi(x,t)\xi(x',t') \rangle &= \sigma^2 \delta(x-x')\delta(t-t') \end{aligned} \tag{7}$$

where σ^2 is a parameter which measures the intensity of the Gaussian white noise and $\delta(\cdot)$ denotes the standard Dirac delta function. To validate the choice of $\xi(x,t)$ as Gaussian white noise, uncorrelated in both time and space, we present in Figures 5 and 6 the histograms of surface height, obtained from 10 000 independent open-loop simulation runs at sufficiently large simulation times, at different positions and times. Specifically, Figure 5 shows the histogram of surface height at different sites ($x = 0a$, $25a$, $50a$, $75a$) at $t = 400$ s, and Figure 6 shows the histogram of surface height at $x = 50a$ for different time instants ($t = 100$, 200, 300, 400 s). It can be clearly seen in Figures 5 and 6 that the surface height follows Gaussian probability distribution at sufficiently large times and that the noise is uncorrelated in both time and space, which indicates that the choice of white noise is a reasonable one.

To proceed with model parameter estimation and control design, a stochastic ODE approximation of eq 4 is first derived using Galerkin's method. Consider the eigenvalue problem of the linear operator of eq 4, which takes the form:

$$A\bar{\phi}_n(x) = \nu \frac{d^2\bar{\phi}_n(x)}{dx^2} = \lambda_n\bar{\phi}_n(x)$$
$$\bar{\phi}_n(-\pi) = \bar{\phi}_n(\pi), \quad \frac{d\bar{\phi}_n}{dx}(-\pi) = \frac{d\bar{\phi}_n}{dx}(\pi) \tag{8}$$

where λ_n denotes an eigenvalue and $\bar{\phi}_n$ denotes an eigenfunction. A direct computation of the solution of the above eigenvalue problem yields $\lambda_0 = 0$ with $\psi_0 = 1/(2\pi)^{1/2}$, and $\lambda_n = -\nu n^2$ (λ_n is an eigenvalue of multiplicity two) with eigenfunctions $\phi_n = (1/\pi^{1/2})\sin(nx)$ and $\psi_n = (1/\pi^{1/2})\cos(nx)$ for $n = 1, ..., \infty$. Note that the $\bar{\phi}_n$ in eq 8 denotes either ϕ_n or ψ_n. For a fixed positive value of ν, all eigenvalues (except the zeroth eigenvalue) are negative, and the distance between two consecutive eigenvalues (i.e., λ_n and λ_{n+1}) increases as n increases.

To this end, the solution of eq 4 is expanded in an infinite series in terms of the eigenfunctions of the operator of eq 8 as follows:

$$h(x,t) = \sum_{n=1}^{\infty}\alpha_n(t)\phi_n(x) + \sum_{n=0}^{\infty}\beta_n(t)\psi_n(x) \tag{9}$$

where $\alpha_n(t)$ and $\beta_n(t)$ are time-varying coefficients. Substituting the above expansion for the solution, $h(x,t)$, into eq 4 and taking the inner product with the adjoint eigenfunctions, $\phi_n^*(x) = (1/\pi^{1/2})\sin(nx)$ and $\psi_n^*(x) = (1/\pi^{1/2})\cos(nx)$, the following system of infinite stochastic ODEs is obtained:

$$\frac{d\beta_0}{dt} = \sqrt{2\pi}r_h + \xi_\beta^0(t)$$
$$\frac{d\alpha_n}{dt} = \lambda_n\alpha_n + \xi_\alpha{}^n(t), \quad \frac{d\beta_n}{dt} = \lambda_n\beta_n + \xi_\beta{}^n(t), \quad n = 1, ..., \infty \tag{10}$$

where

$$\xi_\alpha{}^n(t) = \int_{-\pi}^{\pi}\xi(x,t)\phi_n^*(x)\,dx, \quad \xi_\beta{}^n(t) = \int_{-\pi}^{\pi}\xi(x,t)\psi_n^*(x)\,dx \tag{11}$$

The covariances of $\xi_\alpha{}^n(t)$ and $\xi_\beta{}^n(t)$ can be computed by using the following result:

Result 1: If (1) $f(x)$ is a deterministic function, (2) $\eta(x)$ is a random variable with $\langle\eta(x)\rangle = 0$ and covariance $\langle\eta(x)\eta(x')\rangle = \sigma^2\delta(x - x')$, and (3) $\epsilon = \int_a^b f(x)\eta(x)\,dx$, then ϵ is a real random number with $\langle\epsilon\rangle = 0$ and covariance $\langle\epsilon^2\rangle = \sigma^2\int_a^b f^2(x)\,dx$.[21]

Using result 1, we obtain $\langle\xi_\alpha{}^n(t)\xi_\alpha{}^n(t')\rangle = \sigma^2\delta(t - t')$ and $\langle\xi_\beta{}^n(t)\xi_\beta{}^n(t')\rangle = \sigma^2\delta(t - t')$.

Since the stochastic ODE system is linear, the analytical solution of state variance can be obtained from a direct computation as follows:

$$\langle\alpha_n{}^2(t)\rangle = \frac{\sigma^2}{2\nu n^2} + \left(\langle\alpha_n{}^2(t_0)\rangle - \frac{\sigma^2}{2\nu n^2}\right)e^{-2\nu n^2(t-t_0)}$$
$$\langle\beta_n{}^2(t)\rangle = \frac{\sigma^2}{2\nu n^2} + \left(\langle\beta_n{}^2(t_0)\rangle - \frac{\sigma^2}{2\nu n^2}\right)e^{-2\nu n^2(t-t_0)} \tag{12}$$
$$n = 1, 2, ..., \infty$$

where $\langle\alpha_n{}^2(t_0)\rangle$ and $\langle\beta_n{}^2(t_0)\rangle$ are the state variances at time t_0. The analytical solution of the state variance of eq 12 will be used in the parameter estimation and the MPC design in sections 3.3 and 4.2

When the dynamic model of surface height profile is determined, surface roughness of the thin film is defined as the standard deviation of the surface height profile from its average height and is computed as follows:

$$r(t) = \sqrt{\frac{1}{2\pi}\int_{-\pi}^{\pi}[h(x,t) - \bar{h}(t)]^2\,dx} \tag{13}$$

where $\bar{h}(t) = (1/2\pi)\int_{-\pi}^{\pi}h(x,t)\,dx$ is the average surface height. According to eq 9, we have $\bar{h}(t) = \beta_0(t)\psi_0$. Therefore, $\langle r^2(t)\rangle$ can be rewritten in terms of $\langle\alpha_n{}^2(t)\rangle$ and $\langle\beta_n{}^2(t)\rangle$ as follows:

$$\begin{aligned}\langle r^2(t)\rangle &= \frac{1}{2\pi}\left\langle\int_{-\pi}^{\pi}(h(x,t) - \bar{h}(t))^2\,dx\right\rangle \\ &= \frac{1}{2\pi}\left\langle\int_{-\pi}^{\pi}\left[\sum_{i=1}^{\infty}\alpha_i(t)\phi_i(x) + \sum_{i=0}^{\infty}\beta_i(t)\psi_i(x) - \beta_0(t)\psi_0\right]^2 dx\right\rangle \\ &= \frac{1}{2\pi}\left\langle\int_{-\pi}^{\pi}\sum_{i=1}^{\infty}[\alpha_i{}^2(t)\phi_i{}^2(x) + \beta_i{}^2(t)\psi_i{}^2(x)]\,dx\right\rangle \\ &= \frac{1}{2\pi}\left\langle\sum_{i=1}^{\infty}(\alpha_i{}^2(t) + \beta_i{}^2(t))\right\rangle \\ &= \frac{1}{2\pi}\sum_{i=1}^{\infty}[\langle\alpha_i{}^2(t)\rangle + \langle\beta_i{}^2(t)\rangle]\end{aligned} \tag{14}$$

Thus, eq 14 provides a direct link between the state variance of the infinite stochastic ODEs of eq 10 and the expected surface roughness of the thin film. Note that the model parameter r_h does not appear in the expression of surface roughness, since the zeroth state, β_0, is only affected by r_h, but this state is not included in the computation of the expected surface roughness square of eq 14.

3.2. Deterministic Dynamic Model of Film Site Occupancy Ratio. Since film porosity is another control objective, a dynamic model is necessary in the MPC formulation to describe the evolution of film porosity, which is represented by the film SOR of eq 3. The dynamics of the expected value of the film SOR evolution are approximately described by a linear first-order deterministic ODE as follows:[35]

$$\tau\frac{d\langle\rho(t)\rangle}{dt} = \rho^{ss} - \langle\rho(t)\rangle \tag{15}$$

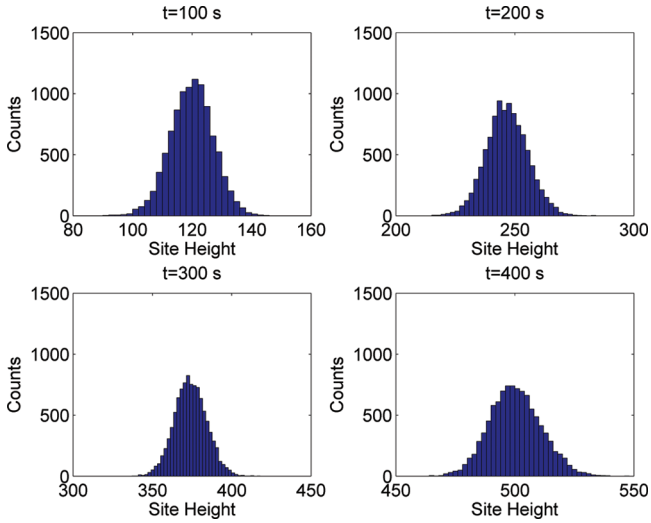

Figure 6. Histogram of surface height at $x = 50a$ for different time instants (t = 100, 200, 300, 400 s).

where t is the time, τ is the time constant, and ρ^{ss} is the steady-state value of the film SOR. The deterministic ODE system of eq 15 is subject to the following initial condition:

$$\langle \rho(t_0) \rangle = \rho_0 \tag{16}$$

where t_0 is the initial time and ρ_0 is the initial value of the film SOR. Note that ρ_0 is a deterministic variable, since ρ_0 refers to the film SOR at $t = t_0$. From eqs 15 and 16, it follows that

$$\langle \rho(t) \rangle = \rho^{ss} + (\rho_0 - \rho^{ss}) e^{-(t-t_0)/\tau} \tag{17}$$

The choice of a deterministic linear ODE for $\langle \rho(t) \rangle$ (eq 15) is made based on open-loop process data, and it adequately describes the dynamics of the film SOR. Validation of the linear model of eq 15 is provided in another work[35] which focuses on porosity control and variance reduction in a deposition process with similar microscopic rules.

3.3. Parameter Estimation. Referring to the EW equation of eq 4 and the deterministic ODE model of eq 15, there are several model parameters, ν, σ^2, ρ^{ss}, and τ, that need to be determined as functions of the substrate temperature. These parameters describe the dynamics of surface height and of film SOR and can be estimated by comparing the predicted evolution profiles for roughness and SOR from the dynamic models of eqs 4 and 15 and the ones from the kMC simulation of the deposition process. Least-square methods are used to estimate the model parameters so that the model predictions are close in a least-squares sense to the kMC simulation data.

Since surface roughness is a control objective, we choose the expected surface roughness square as the output for the parameter estimation of the EW equation of eq 4. Thus, the model coefficients, ν and σ^2 can be obtained by solving the problem of minimizing the prediction of the expected surface roughness square of eq 14 to the one from the kMC simulation at different time instants as follows:

$$\min_{\nu,\sigma^2} \sum_{k=1}^{n_1} \left[\langle r^2(t_k) \rangle - \frac{1}{2\pi} \sum_{i=1}^{\infty} (\langle \alpha_i^2(t_k) \rangle + \langle \beta_i^2(t_k) \rangle) \right]^2 \tag{18}$$

where n_1 is the number of the data samplings of surface height profile and surface roughness from the kMC simulations. The predictions of model state variance, $\langle \alpha_i^2(t_k) \rangle$ and $\langle \beta_i^2(t_k) \rangle$, can be solved from the analytical solution of eq 12.

With respect to the parameters of the equation for film porosity, since the ODE model of eq 15 is linear, ρ^{ss} and τ can be estimated from the solutions of eq 17 by minimizing the sum of the squared difference between the evolution profiles from the ODE model prediction and the kMC simulation at different time instants as follows:

$$\min_{\rho^{ss},\tau} \sum_{k=1}^{n_2} [\langle \rho(t_k) \rangle - (\rho^{ss} + (\rho_0 - \rho^{ss}) e^{-(t_k - t_0)/\tau})]^2 \tag{19}$$

where n_2 is the number of the data pairs, $(t_k, \langle \rho(t_k) \rangle)$, from the kMC simulations.

The data used for the parameter estimation are obtained from the open-loop kMC simulation of the thin film growth process. The process parameters are fixed during each open-loop simulation so that the dependence of the model parameters on the process parameters can be obtained. Due to the stochastic nature of the process, multiple independent simulation runs are performed to obtain the expected values of surface roughness and film SOR.

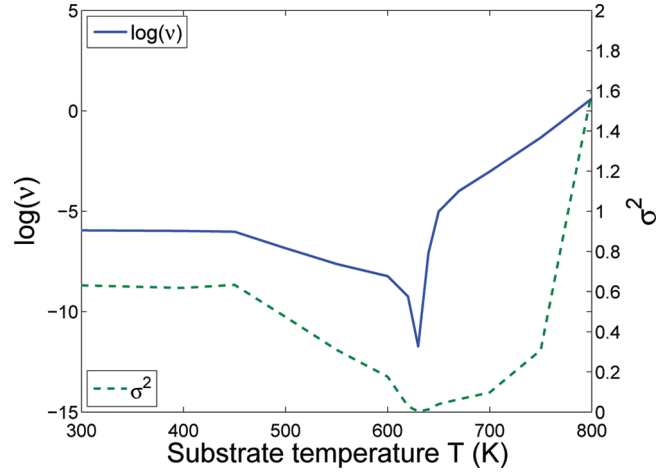

Figure 7. Dependence of $\log(\nu)$ and σ^2 on the substrate temperature with deposition rate $W = 1$ layer/s.

The above parameter estimation process is applied to the open-loop simulation results with 100 lattice size. First, the open-loop evolution profiles of surface roughness and film SOR are obtained from 1000 independent kMC simulation runs with substrate temperature $T = 600$ K and deposition rate $W = 1$ layer/s. Model coefficients are estimated by solving the least-squares problems of eqs 18 and 19 as follows:

$$\rho^{ss} = 0.9823, \quad \tau = 2.9746 \text{ s}, \quad \nu = 2.6570 \times 10^{-4}, \quad \sigma^2 = 0.1757 \tag{20}$$

The EW-type equation with parameters estimated under time-invariant operating conditions is suitable for the purpose of MPC design. This is because the control input in the MPC formulation is piecewise, i.e., the manipulated substrate temperature remains constant between two consecutive sampling times, and thus, the dynamics of the microscopic process can be predicted using the dynamic models with estimated parameters. Eventually, the validation of the constructed models is demonstrated via closed-loop simulations (where the controller which utilizes the approximate models is applied to the kMC simulation of the process) which demonstrate that the desired control objectives are achieved. The simulation results will be shown in section 5 below.

The dependence of the model coefficients on substrate temperature is used in the formulation of the model predictive controller in the next section. Thus, parameter estimation from open-loop kMC simulation results of the thin film growth process for a variety of operation conditions is performed to obtain the dependence of the model coefficients on substrate temperature. In this work, the deposition rate for all simulations is fixed at 1 layer/s. The range of T is between 300 and 800 K, which is from room temperature to the upper limit of the allowable temperature for a valid on-lattice kMC model of silicon film. The dependence of the model parameters on the substrate temperature is shown in Figures 7 and 8. In these figures, it can be clearly seen that the dependence of the model parameters on temperature is highly nonlinear. Specifically, as substrate temperature increases, the migration rate becomes larger due to the Arrhenius-type dependence of the migration rate on temperature. Thus, higher temperature tends to result in a thin film with less pores (higher film SOR) and a smoother surface (lower surface roughness).

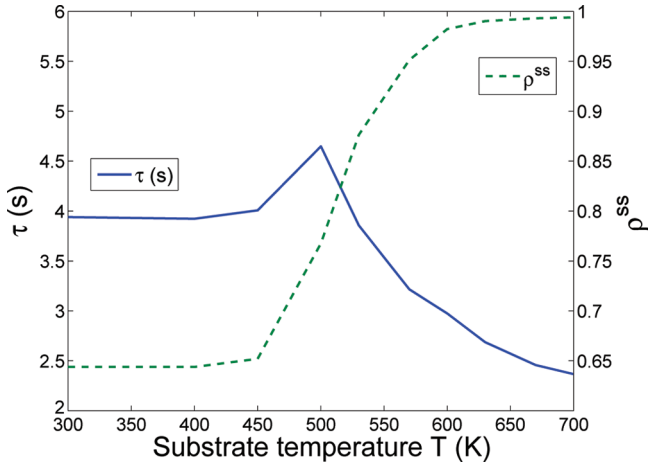

Figure 8. Dependence of ρ^{ss} and τ on the substrate temperature with deposition rate $W = 1$ layer/s.

4. Model Predictive Control

In this section, we design a model predictive controller based on the dynamic models of surface roughness and film SOR to simultaneously control the expected values of roughness square and film SOR to a desired level. The dynamics of surface roughness of the thin film are described by the EW equation of the surface height of eq 4 with appropriately computed parameters. Film SOR is modeled by a first-order deterministic ODE model. State feedback control is considered in this work, i.e., the surface height profile and the value of film SOR are assumed to be available to the controller and no sensor noise is introduced. Measurements of the film may be obtained in real-time through a combination of real-time gas phase measurements and empirical models that predict film porosity from gas phase measurements.

4.1. MPC Formulation for Regulation of Roughness and Porosity. We consider the problem of regulation of surface roughness and of film SOR to desired levels within a model predictive control framework. Since surface roughness and film SOR are stochastic variables, the expected values, $\langle r^2(t)\rangle$ and $\langle\rho\rangle$, are chosen as the control objectives. The substrate temperature is used as the manipulated input and the deposition rate is fixed at a certain value, W_0, during the entire closed-loop simulation. To account for a number of practical considerations, several constraints are added to the control problem. First, there is a constraint on the range of variation of the substrate temperature. This constraint ensures validity of the on-lattice kMC model. Another constraint is imposed on the rate of change of the substrate temperature to account for actuator limitations. The control action at time t is obtained by solving a finite-horizon optimal control problem. The cost function in the optimal control problem includes penalty on the deviation of $\langle r^2\rangle$ and $\langle\rho\rangle$ from their respective set-point values. Different weighting factors are assigned to the penalties of the surface roughness and of the film SOR. Surface roughness and film SOR have very different magnitudes, ($\langle r^2\rangle$ ranges from 1 to 10^2 and $\langle\rho\rangle$ ranges from 0 to 1). Therefore, relative deviations are used in the formulation of the cost function to make the magnitude of the two terms comparable. The optimization problem is subject to the dynamics of the surface height of eq 4 of and of the film SOR of eq 15. The optimal temperature profile is calculated by solving a finite-dimensional optimization problem in a receding horizon fashion. Specifically, the MPC problem is formulated as follows:

$$\min_{T_1,\ldots,T_i,\ldots,T_p} J = \sum_{i=1}^{p}\left\{q_{r^2,i}\left[\frac{r_{set}^{\ 2} - \langle r^2(t_i)\rangle}{r_{set}^{\ 2}}\right]^2 + q_{\rho,i}\left[\frac{\rho_{set} - \langle\rho(t_i)\rangle}{\rho_{set}}\right]^2\right\}$$

subject to

$$\frac{\partial h}{\partial t} = r_h + \nu\frac{\partial^2 h}{\partial x^2} + \xi(x,t)$$

$$\tau\frac{d\langle\rho(t)\rangle}{dt} = \rho^{ss} - \langle\rho(t)\rangle$$

$$T_{min} < T_i < T_{max}, \quad \left|\frac{T_{i+1} - T_i}{\Delta}\right| \le L_T$$

$$i = 1, 2, \ldots, p \tag{21}$$

where t is the current time, Δ is the sampling time, p is the number of prediction steps, $p\Delta$ is the specified prediction horizon, t_i, $i = 1, 2, \ldots, p$, is the time of the ith prediction step ($t_i = t + i\Delta$), respectively, T_i, $i = 1, 2, \ldots, p$, is the substrate temperature at the ith step ($T_i = T(t + i\Delta)$), respectively, W_0 is the fixed deposition rate, $q_{r^2,i}$ and $q_{\rho,i}$, $i = 1, 2, \ldots, p$, are the weighting penalty factors for the deviations of $\langle r^2\rangle$ and $\langle\rho\rangle$ from their respective set-points at the ith prediction step, T_{min} and T_{max} are the lower and upper bounds on the substrate temperature, respectively, and L_T is the limit on the rate of change of the substrate temperature.

The optimal set of control actions, ($T_1, T_2, \ldots, T_p$), is obtained from the solution of the multivariable optimization problem of eq 21, and only the first value of the manipulated input trajectory, T_1, is applied to the deposition process (i.e., kMC model) during the time interval (t, $t + \Delta$). At time $t + \Delta$, new measurements of ρ and h are received and the MPC problem of eq 21 is solved for the next control input trajectory.

4.2. MPC Formulation Based on a Reduced-Order Model. The MPC formulation proposed in eq 21 is developed on the basis of the EW equation of surface height and the deterministic ODE model of the film SOR. The EW equation, which is a distributed parameter dynamic model, contains infinite dimensional stochastic states. Therefore, it leads to a model predictive controller of infinite order that cannot be realized in practice (i.e., the practical implementation of such a control algorithm will require the computation of infinite sums which cannot be done by a computer). To this end, a finite dimensional approximation of the EW equation of order $2m$ is used; this approximation is obtained by using the first $2m$ modes in eq 10.

Due to the structure of the eigenspectrum of the linear operator of the EW equation of eq 4, the dynamics of the EW equation are characterized by a finite number of dominant modes. By neglecting the high-order modes ($n \ge m + 1$), we rewrite the system of eq 10 into a finite-dimensional approximation as follows:

$$\frac{d\alpha_n}{dt} = \lambda_n\alpha_n + \xi_\alpha^{\ n}(t) \quad n = 1, \ldots, m$$
$$\frac{d\beta_n}{dt} = \lambda_n\beta_n + \xi_\beta^{\ n}(t) \quad n = 1, \ldots, m \tag{22}$$

Using the finite-dimensional system of eq 22, the expected surface roughness square, $\langle r^2(t)\rangle$, can be approximated with the finite-dimensional state variance as follows:

$$\langle\tilde{r}^2(t)\rangle = \frac{1}{2\pi}\sum_{i=1}^{m}[\langle\alpha_i^{\ 2}(t)\rangle + \langle\beta_i^{\ 2}(t)\rangle] \tag{23}$$

where the tilde symbol in $\langle\tilde{r}^2(t)\rangle$ denotes its association with a finite-dimensional system.

Thus, the MPC formulation on the basis of the finite-dimensional system of eq 22 and of the expected film SOR of eq 17 is shown as follows:

$$\min_{T_1,\ldots,T_i,\ldots,T_p} J = \sum_{i=1}^{p}\left\{q_{r^2,i}\left[\frac{r_{\text{set}}^{\,2} - \langle \tilde{r}^2(t_i)\rangle}{r_{\text{set}}^{\,2}}\right]^2 + q_{\rho,i}\left[\frac{\rho_{\text{set}} - \langle\rho(t_i)\rangle}{\rho_{\text{set}}}\right]^2\right\}$$

subject to

$$\langle \alpha_n^{\,2}(t_i)\rangle = \frac{\sigma^2}{2\nu n^2} + \left(\langle \alpha_n^{\,2}(t_{i-1})\rangle - \frac{\sigma^2}{2\nu n^2}\right)e^{-2\nu n^2\Delta}$$

$$\langle \beta_n^{\,2}(t_i)\rangle = \frac{\sigma^2}{2\nu n^2} + \left(\langle \beta_n^{\,2}(t_{i-1})\rangle - \frac{\sigma^2}{2\nu n^2}\right)e^{-2\nu n^2\Delta}$$

$$\langle\rho(t_i)\rangle = \rho^{ss} + (\langle\rho(t_{i-1})\rangle - \rho^{ss})e^{-\Delta/\tau}$$

$$T_{\min} < T_i < T_{\max}, \quad \left|\frac{T_{i+1} - T_i}{\Delta}\right| \le L_T$$

$$n = 1, 2, \ldots, m \quad i = 1, 2, \ldots, p \tag{24}$$

In the MPC formulation based on the reduced-order model of eq 24, the expected value of film SOR, $\langle\rho\rangle$, and the variance of the modal states, $\langle \alpha_n^{\,2}(t)\rangle$ and $\langle \beta_n^{\,2}(t)\rangle$, are needed to calculate the variables included in the cost over the prediction horizon. In the closed-loop simulations, the instantaneous values of ρ, $\alpha_n^{\,2}(t)$, and $\beta_n^{\,2}(t)$ are made available to the controller at each sampling time; however, no statistical information, e.g., the expected value and variances, is available for feedback. Therefore, these instantaneous values at the sampling times, which are obtained directly from the simulation in real-time, are considered as the expected value of film SOR and height and the variances of the modal states and can be used as initial conditions for the solution of the dynamic models employed in the MPC formulation of eq 24. Specifically, $\alpha_n^{\,2}(t)$ and $\beta_n^{\,2}(t)$ are computed from the surface height profile by taking the inner product with the adjoint eigenfunctions as follows:

$$\alpha_n(t) = \int_{-\pi}^{\pi} h(x,t)\phi_n^*(x)\,dx$$

$$\beta_n(t) = \int_{-\pi}^{\pi} h(x,t)\psi_n^*(x)\,dx \qquad n = 1, 2, \ldots, m \tag{25}$$

where $h(x,t)$ is obtained at each sampling time from the kMC simulation.

5. Simulation Results

In this section, the proposed model predictive controller of eq 24 is applied to the kMC model of the thin film growth process described in section 2. The value of the substrate temperature is obtained from the solution of the problem of eq 24 at each sampling time and is applied to the closed-loop system until the next sampling time. The optimization problem in the MPC formulation of eq 24 is solved via a local constrained minimization algorithm using a broad set of initial guesses.

The constraint on the rate of change of the substrate temperature is imposed onto the optimization problem, which is realized in the optimization process in the following way:

$$\left|\frac{T_{i+1} - T_i}{\Delta}\right| \le L_T \Rightarrow |T_{i+1} - T_i| \le L_T\Delta \Rightarrow$$

$$T_i - L_T\Delta \le T_{i+1} \le T_i + L_T\Delta \qquad i = 1, 2, \ldots, p \tag{26}$$

The desired values (set-point values) in the closed-loop simulations are $r_{\text{set}}^{\,2} = 10.0$ and $\rho_{\text{set}} = 0.95$. The order of finite-dimensional approximation of the EW equation in the MPC formulation is $m = 20$. The deposition rate is fixed at 1 layer/s and an initial temperature of 600 K is used. The variation of temperature is from 400 to 700 K. The maximum rate of change of the temperature is $L_T = 10$ K/s. The sampling time is fixed at $\Delta = 1$ s. The number of prediction steps is set to be $p = 5$. The closed-loop simulation duration is 1000 s. All expected values are obtained from 1000 independent simulation runs.

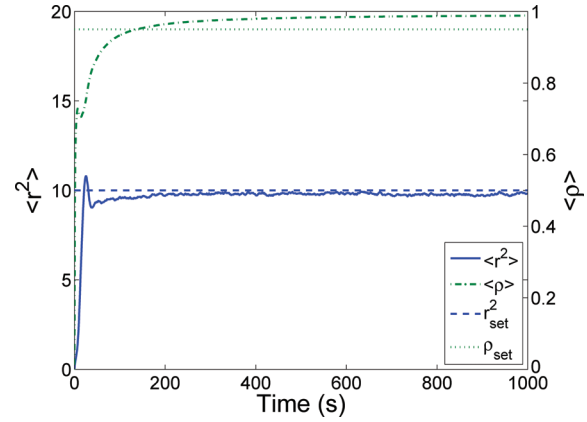

Figure 9. Profiles of the expected values of surface roughness square (solid line) and of the film SOR (dash-dotted line) under closed-loop operation with a cost function including only a penalty on surface roughness.

The estimated parameters and the dependence of the parameters on substrate temperature is used in the model predictive control design, which is applied to the kMC simulations with the same lattice size, $L = 100$. We note that the 100 lattice size in the kMC simulations is small compared to real wafers in the deposition process. However, it is not possible with currently available computing power to simulate molecular processes covering a realistic wafer size. However, developing modeling and control techniques for regulating thin film microstructure (surface roughness and porosity) is an important research area because we need to understand how to regulate film surface roughness and porosity in industrial systems. The proposed modeling and control methods can be applied to any lattice size. Furthermore, the dynamic models used in the controller can be constructed directly from experimental surface roughness and porosity measurements.

Closed-loop simulations of separately regulating film surface roughness and porosity are first carried out. In these control problems, the control objective is to regulate one of the control variables, i.e., either surface roughness or film SOR, to a desired level. The cost functions of these problems contain only penalty on the error of the expected surface roughness square or of the expected film SOR from their set-point values. The corresponding MPC formulations can be realized by assigning different values to the penalty weighting factors, $q_{r^2,i}$ and $q_{\rho,i}$.

In the roughness-only control problem, the weighting factors take the following values: $q_{r^2,i} = 1$ and $q_{\rho,i} = 0$, $i = 1, 2, \ldots, p$. Figures 9 and 10 show the closed-loop simulation results of the roughness-only control problem. From Figure 9, we can see that the expected surface roughness square is successfully regulated at the desired level, 10. Since no penalty is included on the error of the expected film SOR, the final value of expected film SOR at the end of the simulation, $t = 1000$ s, is 0.988, which is far from the desired film SOR, 0.95.

In the SOR-only control problem, the weighting factors are assigned as: $q_{r^2,i} = 0$ and $q_{\rho,i} = 1$, $i = 1, 2, \ldots, p$. Figures 10 and 11 show the closed-loop simulation results of the SOR-only control problem. Similar to the results of the roughness-only control problem, the desired value of expected film SOR,

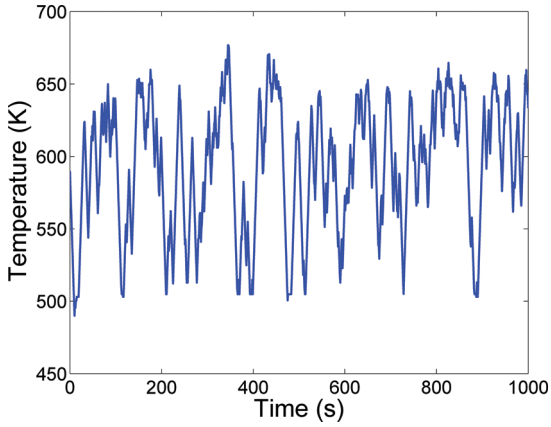

Figure 10. Profile of the instantaneous substrate temperature under closed-loop operation with a cost function including only a penalty on surface roughness.

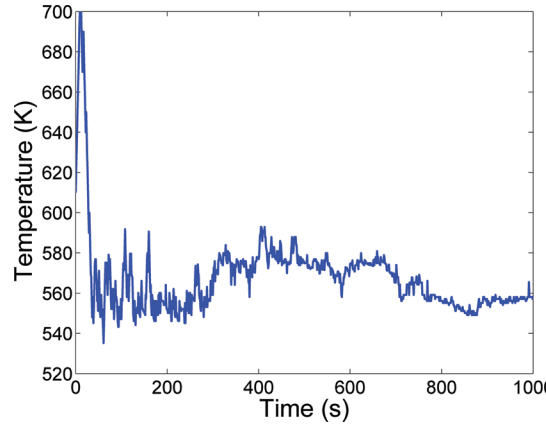

Figure 12. Profile of the instantaneous substrate temperature under closed-loop operation with a cost function including only a penalty on the film SOR.

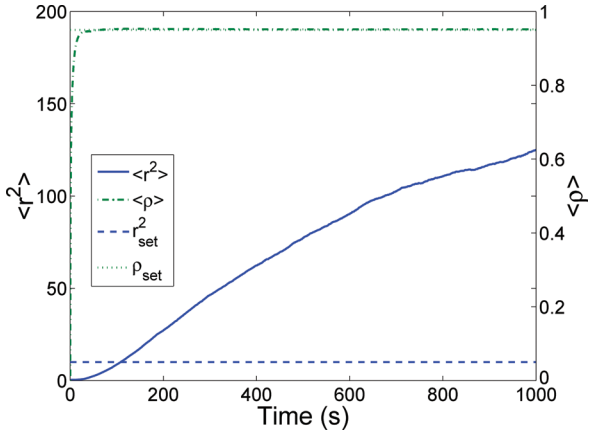

Figure 11. Profiles of the expected values of surface roughness square (solid line) and of the film SOR (dashed−dotted line) under closed-loop operation with a cost function including only a penalty on the film SOR.

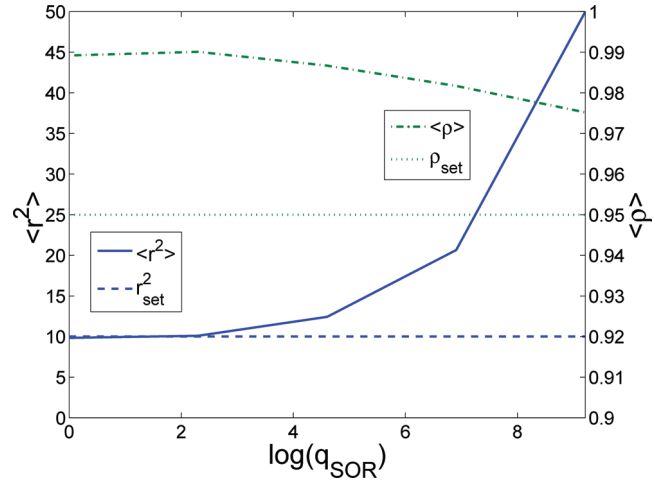

Figure 13. Profiles of the expected values of surface roughness square (solid line) and of the film SOR (dashed−dotted line) at the end of the closed-loop simulations ($t = 1000$ s) with the following penalty weighting factors: $q_{r^2,i}$ fixed at 1 for all i and for different values of q_{SOR}.

0.95, is approached at large times. However, since the error from the expected surface roughness square is not considered in the cost function, $\langle r^2 \rangle$ reaches a very high level around 125 at the end of the simulation.

Finally, closed-loop simulations of simultaneous regulation of surface roughness and film SOR are carried out by assigning nonzero values to both penalty weighting factors. Specifically, $q_{r^2,1} = q_{r^2,2} = ... = q_{r^2,p} = 1$ and $q_{\rho,1} = q_{\rho,2} = ... = q_{\rho,p} = q_{SOR}$, and q_{SOR} varies from 1 to 10^4. Since substrate temperature is the only manipulated input, the desired values of r_{set}^2 and ρ_{set} cannot be achieved simultaneously. With different assignments of penalty weighting factors, the model predictive controller of eq 24 evaluates and strikes a balance between the two set-points. Figure 13 shows the expected values of r_{set}^2 and ρ_{set} at the end of closed-loop simulations of the simultaneous control problem with respect to different weighting factors. It is clear from Figure 13 that as the weighting on expected film SOR increases, the expected film SOR approaches its set-point value of 0.95, while the expected surface roughness square deviates from its set-point value of 10.

Snapshots of the film microstructure at the end of the simulations (i.e., $t = 1000$ s) under open-loop and closed-loop operations are shown in Figure 14. The open-loop simulation is carried out at fixed process parameters of substrate temperature, 500 K, and adsorption rate, 1.0 layer/s. The thin film obtained at the end of the open-loop simulation has higher surface roughness and film porosity, with the expected values of surface roughness square at 106 and film SOR at 0.78. Columnar/pillar structures can be seen in the film microstructure in the open-loop simulation (Figure 14). Similar columnar structures have been also reported by other researchers in kMC simulations with a triangular lattice and similar microscopic rules as well as in experimental works.[36,43,31]

In the closed-loop simulations shown in Figure 14, three control schemes are compared: roughness-only control (I), SOR-only control (II), and simultaneous regulation of both roughness and porosity (III). As it was demonstrated by the evolution profiles of surface roughness and film SOR of the closed-loop simulations in Figures 9 and 11, the film microstructure under roughness-only control (I) has the lowest surface roughness square, which is close to the set-point value of 10.0, but the corresponding film SOR is 0.99, which is far from the desired value of 0.95. On the other hand, the film SOR under SOR-only control (II) is lower than under roughness-only control (I) and reaches the set-point of 0.95, which can be also seen by comparing the porosity of the thin film under closed-loop control (I and II) in Figure 14. However, the surface roughness square under SOR-only control (II) is much higher than the set-point value of 10.0 since no penalty is included on the deviation of surface roughness square from the set-point value in this case,

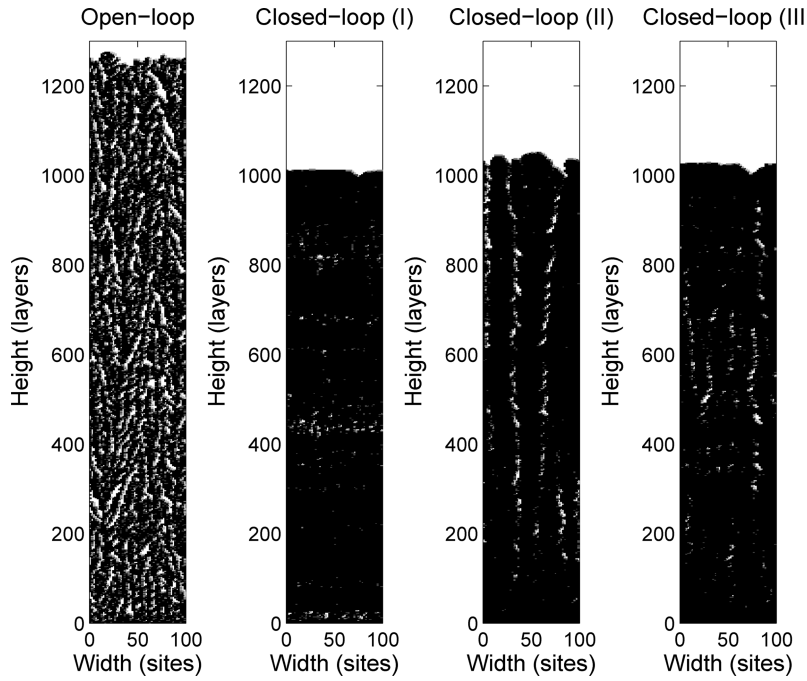

Figure 14. Snapshots of the film microstructure at the end ($t = 1000$ s) of simulations under open-loop and closed-loop operations. Open-loop simulation is carried out at $T = 500$ K and $W = 1.0$ layer/s. Closed-loop simulations are carried out under three different control schemes: (I) roughness-only control; (II) SOR-only control; (III) simultaneous regulation of surface roughness and film SOR with $q_{r^2,i} = 1$ and $q_{SOR} = 10\,000$.

and thus, the snapshot of the film microstructure has the roughest surface. Finally, under control scheme III, surface roughness and film porosity strike a balance from their respective set-points by including a penalty on both deviations of surface roughness square and film SOR.

Remark 1. The thin film growth process is a batch process and the process objective, addressed in the present work, is to produce a thin film at the end of the batch that meets specific surface roughness and internal porosity requirements using substrate temperature as the manipulated input. The initial state of the deposition system (at time $t = 0$) is to consider a clean initial surface and a nominal initial temperature; both choices are natural for a deposition process, and as can be clearly seen in Figures 10 and 12, the substrate temperature varies significantly and in a highly nonlinear fashion from its initial value. Thus, it is not possible to improve the closed-loop performance with a better choice of the initial substrate temperature or by using a constant substrate temperature. Then, the objective of the model predictive controller is to compute in real-time the substrate temperature profile (subject to magnitude and rate of change constraints) needed to produce a thin film with the desired surface roughness and internal porosity requirements at the end of the batch. It is also important to note that the proposed reduced-order modeling and MPC strategy can be readily used off-line to compute a recipe for varying the substrate temperature with respect to time (simply set the MPC prediction horizon equal to the entire deposition time) and then the MPC can be used in real-time to correct this input trajectory. Note here that if the optimization problem for computing the time-varying policy for the substrate temperature is formulated on the basis of the kinetic Monte Carlo model of the deposition process, it leads to dynamic optimization problems with intractable computational times for their solution (on the order of months) and this is where the true value of the reduced-order models used in the MPC lies. Finally, in the absence of real-time measurements, the MPC strategy can be still be used in an open-loop fashion to compute the operating policy for the substrate temperature.

6. Conclusions

In this work, stochastic modeling and simultaneous regulation of surface roughness and film porosity was studied for a porous thin film deposition process modeled via kMC simulation on a triangular lattice with two microscopic processes. The definition of surface height profile of a porous thin film in a triangular lattice was first introduced. An EW-type equation was used to describe the dynamics of surface height and the evolution of the RMS surface roughness, which is one of the controlled variables. Subsequently, an appropriate definition of film SOR was introduced to represent the extent of porosity inside the film and was used as the second to-be-controlled variable. A deterministic ODE model was postulated to describe the time evolution of film SOR. The coefficients of the EW equation of surface height and of the deterministic ODE model of the film SOR were estimated on the basis of data obtained from the kMC simulator of the deposition process using least-squares methods, and their dependence on substrate temperature was determined. The developed dynamic models were used as the basis for the design of a model predictive control algorithm that includes a penalty on the deviation of surface roughness square and film SOR from their respective set-point values. Simulation results demonstrated the applicability and effectiveness of the proposed modeling and control approach in the context of the deposition process under consideration. When simultaneous control of surface roughness and porosity was carried out, a balanced trade-off was obtained in the closed-loop system between the two control objectives of surface roughness and porosity regulation.

Acknowledgment

Financial support from NSF, CBET-0652131, is gratefully acknowledged.

Literature Cited

(1) Zapien, J. A.; Messier, R.; Collin, R. W. Ultraviolet-extended real-time spectroscopic ellipsometry for characterization of phase evolution in BN thin films. *Appl. Phys. Lett.* **2001**, *78*, 1982–1984.

(2) Renaud, G.; Lazzari, R.; Revenant, C.; et al. Real-time monitoring of growing nanoparticles. *Science* **2003**, *300*, 1416–1419.

(3) Buzea, C.; Robbie, K. State of the art in thin film thickness and deposition rate monitoring sensors. *Rep. Prog. Phys.* **2005**, *68*, 385–409.

(4) Lou, Y.; Christofides, P. D. Estimation and control of surface roughness in thin film growth using kinetic Monte-Carlo models. *Chem. Eng. Sci.* **2003**, *58*, 3115–3129.

(5) Lou, Y.; Christofides, P. D. Feedback control of growth rate and surface roughness in thin film growth. *AIChE J.* **2003**, *49*, 2099–2113.

(6) Christofides, P. D.; Armaou, A.; Lou, Y.; Varshney, A. *Control and Optimization of Multiscale Process Systems*; Birkhäuser: Boston, 2008.

(7) Lou, Y.; Christofides, P. D. Feedback control of surface roughness of GaAs (001) thin films using kinetic Monte Carlo models. *Comput. Chem. Eng.* **2004**, *29*, 225–241.

(8) Ni, D.; Christofides, P. D. Dynamics and control of thin film surface microstructure in a complex deposition process. *Chem. Eng. Sci.* **2005**, *60*, 1603–1617.

(9) Varshney, A.; Armaou, A. Multiscale optimization using hybrid PDE/kMC process systems with application to thin film growth. *Chem. Eng. Sci.* **2005**, *60*, 6780–6794.

(10) Siettos, C. I.; Armaou, A.; Makeev, A. G.; Kevrekidis, I. G. Microscopic/stochastic timesteppers and "coarse" control: A kMC example. *AIChE J.* **2003**, *49*, 1922–1926.

(11) Armaou, A.; Siettos, C. I.; Kevrekidis, I. G. Time-steppers and 'coarse' control of distributed microscopic processes. *Int. J. Robust Nonlin. Control* **2004**, *14*, 89–111.

(12) Varshney, A.; Armaou, A. Identification of macroscopic variables for low-order modeling of thin-film growth. *Ind. Eng. Chem. Res.* **2006**, *45*, 8290–8298.

(13) Edwards, S. F.; Wilkinson, D. R. The surface statistics of a granular aggregate. *Proc. R. Soc. London Ser. A—Math. Phys. Eng. Sci.* **1982**, *381*, 17–31.

(14) Villain, J. Continuum models of crystal growth from atomic beams with and without desorption. *J. Phys. I* **1991**, *1*, 19–42.

(15) Vvedensky, D. D.; Zangwill, A.; Luse, C. N.; Wilby, M. R. Stochastic equations of motion for epitaxial growth. *Phys. Rev. E* **1993**, *48*, 852–862.

(16) Cuerno, R.; Makse, H. A.; Tomassone, S.; Harrington, S. T.; Stanley, H. E. Stochastic model for surface erosion via ion sputtering: Dynamical evolution from ripple morphology to rough morphology. *Phys. Rev. Lett.* **1995**, *75*, 4464–4467.

(17) Lauritsen, K. B.; Cuerno, R.; Makse, H. A. Noisy Kuramote-Sivashinsky equation for an erosion model. *Phys. Rev. E* **1996**, *54*, 3577–3580.

(18) Kardar, M.; Parisi, G; Zhang, Y. C. Dynamic scaling of growing. *Interfaces Phys. Rev. Lett.* **1986**, *56*, 889–892.

(19) Ballestad, A.; Ruck, B. J.; Schmid, J. H.; et al. Surface morphology of GaAs during molecular beam epitaxy growth: Comparison of experimental data with simulations based on continuum growth equations. *Phys. Rev. B* **2002**, *65*, 205302.

(20) Kan, H. C.; Shah, S.; Tadyyon-Eslami, T.; Phaneuf, R. J. Transient evolution of surface roughness on patterned GaAs(001) during homoepitaxial growth. *Phys. Rev. Lett.* **2004**, *92*, 146101.

(21) Åström, K. J. *Introduction to Stochastic Control Theory*; Academic Press: New York, 1970.

(22) Bohlin, T.; Graebe, S. F. Issues in nonlinear stochastic grey-box identification. *Int. J. Adaptive Control Signal Process.* **1995**, *9*, 465–490.

(23) Kristensen, N. R.; Madsen, H.; Jorgensen, S. B. Parameter estimation in stochastic grey-box models. *Automatica* **2004**, *40*, 225–237.

(24) Ni, D.; Christofides, P. D. Multivariable predictive control of thin film deposition using a stochastic PDE model. *Ind. Eng. Chem. Res.* **2005**, *44*, 2416–2427.

(25) Lou, Y.; Christofides, P. D. Feedback control of surface roughness in sputtering processes using the stochastic Kuramoto-Sivashinsky equation. *Comput. Chem. Eng.* **2005**, *29*, 741–759.

(26) Lou, Y.; Christofides, P. D. Nonlinear feedback control of surface roughness using a stochastic PDE: Design and application to a sputtering process. *Ind. Eng. Chem. Res.* **2006**, *45*, 7177–7189.

(27) Hu, G.; Lou, Y.; Christofides, P. D. Model parameter estimation and feedback control of surface roughness in a sputtering process. *Chem. Eng. Sci.* **2008**, *63*, 1810–1816.

(28) Lou, Y.; Christofides, P. D. Feedback control of surface roughness using stochastic PDEs. *AIChE J.* **2005**, *51*, 345–352.

(29) Hu, G.; Lou, Y.; Christofides, P. D. Dynamic output feedback covariance control of stochastic dissipative partial differential equations. *Chem. Eng. Sci.* **2008**, *63*, 4531–4542.

(30) Lou, Y.; Hu, G.; Christofides, P. D. Model predictive control of nonlinear stochastic partial differential equations with application to a sputtering process. *AIChE J.* **2008**, *54*, 2065–2081.

(31) Wang, L.; Clancy, P. A kinetic Monte Carlo study of the growth of Si on Si(100) at varying angles of incident deposition. *Surf. Sci.* **1998**, *401*, 112–123.

(32) Zhang, P.; Zheng, X.; Wu, S.; Liu, J.; He, D. Kinetic Monte Carlo simulation of Cu thin film growth. *Vacuum* **2004**, *72*, 405–410.

(33) Levine, S. W.; Clancy, P. A simple model for the growth of polycrystalline Si using the kinetic Monte Carlo simulation. *Modell. Simul. Mater. Sci. Eng.* **2000**, *8*, 751–762.

(34) Wang, L.; Clancy, P. Kinetic Monte Carlo simulation of the growth of polycrystalline Cu films. *Surf. Sci.* **2001**, *473*, 25–38.

(35) Hu, G.; Orkoulas, G.; Christofides, P. D. Modelling and control of film porosity in thin film deposition. *Chem. Eng. Sci.*, DOI: 10.1016/j.ces.2009.05.008.

(36) Yang, Y. G.; Johnson, R. A.; Wadley, H. N. A Monte Carlo simulation of the physical vapor deposition of nickel. *Acta Mater.* **1997**, *45*, 1455–1468.

(37) Keršulis, S.; Mitin, V. Monte Carlo simulation of growth and recovery of silicon. *Mater. Sci. Eng. B* **1995**, *29*, 34–37.

(38) Makov, G.; Payne, M. C. Periodic boundary conditions in ab initio calculations. *Phys. Rev. B* **1995**, *51*, 4014–4022.

(39) Ziff, R. M.; Gulari, E.; Barshad, Y. Kinetic phase transitions in an irreversible surface-reaction model. *Phys. Rev. Lett.* **1986**, *56*, 2553–2556.

(40) Maksym, P. B. Fast Monte Carlo simulation of MBE growth. *Semicond. Sci. Technol.* **1988**, *3*, 594–596.

(41) Vlachos, D. G.; Schmidt, L. D.; Aris, R. Kinetics of faceting of crystals in growth, etching, and equilibrium. *Phys. Rev. B* **1993**, *47*, 4896–4909.

(42) Reese, J. S.; Raimondeau, S.; Vlachos, D. G. Monte Carlo algorithms for complex surface reaction mechanisms: Efficiency and accuracy. *J. Comput. Phys.* **2001**, *173*, 302–321.

(43) Yang, Y. G.; Hass, D. D.; Wadley, H. N. Porosity control in zig-zag vapor-deposited films. *Thin Solid Films* **2005**, *471*, 1–11.

Received for review January 5, 2009
Accepted June 1, 2009

IE900708V